

Supporting Information

Manka et al.

SI Materials and Methods

Preparation of MMP-1 derivatives. ProMMP-1(E200A) (N-terminus of prodomain is number 1), the Hpx domain of MMP-1 (252-447), proMMP-1Cat(E200A) (1-242), and the proforms of the active MMP-1 variants were constructed using standard PCR methods, cloned in the pET3a vector, overexpressed in *E. coli* BL21 DE3, refolded from inclusion bodies and purified as described previously (1). ProMMPs were activated with a catalytic domain of MMP-3 in a 50:1 molar ratio and 1 mM 4-aminophenyl mercuric acetate in TNC buffer (50 mM Tris-HCl pH 7.5, 150 mM NaCl, 10 mM CaCl₂, 0.02 % NaN₃) for 60-120 min at 37 °C. The mature forms were finally purified by Sephacryl S-200 gel filtration (GE Healthcare).

Purification of collagen I. Type I collagen was extracted from Guinea pig dermis. The skin was extensively scraped, cut into pieces, washed with saline, extracted with 0.5 M acetic acid with pepsin added to 1/50 of the total wet weight for 24 h at 4 °C, and collagen was purified as described (2). Yield was determined after freeze-drying.

Synthesis of collagen peptides. A series of triple-helical collagen peptides that collectively represent the whole molecule of human collagen II (Toolkit II) as well as mutant peptides (Fig. S2A) and the peptide used for co-crystallization with MMP-1(E200A) were synthesized by Fmoc (*N*-(9-fluorenyl)methoxycarbonyl) chemistry as C-terminal amides on TentaGel R RAM resin in an Applied Biosystems Pioneer automated synthesizer and purified as described (3). Every peptide in the Toolkit contains 27 amino acids of collagen II (so called “guest” sequence), with 9 amino acid overlap between the neighbouring peptides, flanked by 5 GPP repeats and a GPC knot (“host” sequences) that impart triple-helical conformation on the whole peptide. For exact sequences see (4). All peptides were verified by mass spectrometry and shown to adopt triple-helical conformation by polarimetry.

Collagen I and collagen peptide binding assays. Proteins in 50 mM (CHES) buffer pH 8.8 containing 200 mM NaCl and 10 mM CaCl₂ were reacted with EZ link LC-NHS biotin (Sigma) in water at a final 1:2 protein:biotin molar ratio for 1 h at room temperature. Excess biotin was removed by Sephadex G-25M PD-10 column (GE Healthcare) equilibrated in TNC buffer. The biotinylation did not affect collagenase activity of active MMP-1 and collagen unfolding activity (5) of MMP-1(E200A). For collagen binding assay, Costar® High Binding 96-well microtiter plates (Corning, UK) were coated with 50 µl of 20 µg/ml collagen I in TNC buffer, overnight at room temperature. They were washed with TNC buffer containing 0.05 % Tween 20 (TNC-T) and blocked with 3 % bovine serum albumin (Sigma) in TNC-T buffer. Biotinylated proteins at increasing concentrations were added in TNC buffer and incubated for 2 h at 4-40 °C. The wells were then washed in TNC-T buffer at the temperature of incubation and in temperature-dependent binding experiments they were then fixed with 3 % p-formaldehyde for 30 min.

The fixing step was omitted in room temperature binding experiments. Plates were developed using streptavidin-horseradish peroxidase conjugate (R&D, UK) and 3,3',5,5'-tetramethylbenzidine 2-Component Microwell Peroxidase Substrate Kit™ (KPL, UK) for a fixed time. For the collagen peptide library (Toolkit II) screening the Costar plates were coated with a 5 µg/ml collagen peptide solution in 10 mM acetic acid, incubated overnight at 4 °C, washed and blocked as described above. Biotinylated proteins at 1 µM concentration were added and incubated 1-2 h at room temperature. Plates were developed as in the collagen binding assay. All assays were carried out in a triplicate and compared analyses were always developed simultaneously.

H/DXMS experiment. We first established a peptic peptide mass mapping of MMP-1(E200A) which was essential for H/D exchange localization. MMP-1(E200A) was digested with pepsin by passing through a homemade 2.1 x 50 mm pepsin column based on POROS AL20 material (Applied Biosystems) and the peptic fragments were separated on a 2.1 x 250 mm C18 column (Grace/Vydac). The C18 fractions were subjected to nano-LC-ESI and MALDI MS/MS analyses (Waters). The combined peptide mapping covered 84% of MMP-1(E200A) sequence (Table S1). For H/D exchange analyses 15 µM MMP-1(E200A) was incubated with or without 20 µM collagen I at 25 °C for 1 h in 25 mM MOPS buffer containing 150 mM NaCl and 10 mM CaCl₂ (H₂O-MOPS-NC) pH7.5 and diluted 5-fold into 25 mM D₂O-MOPS-NC pD7.5, so that the final D₂O content was 80 %. Samples were collected from the H/D exchange reaction mix at various timepoints (5 s – 5 h), cooled to 0 °C, acidified to pH 2.5 by addition of concentrated formic acid, and immediately passed through the pepsin column, followed by a 2.1 x 20 mm POROS R1 (Applied Biosystems) trap column. The resultant peptides were then immediately separated on a 2.1 x 50 mm C18 column (Grace/Vydac) at 1 °C and eluted directly into the Micromass Q-TOF mass spectrometer (Waters). Deuterium exchanged spectra were assigned using the catalogue of MMP-1 peptic peptides (Table S1). Natural isotopic patterns of assigned MMP-1(E200A) peptides as well as those of each time-point of H/D exchange reaction were found in total ion chromatograms and identified in MS spectra by manual inspection. Centroid (average) mass of each isotopic pattern was computed using HX-Express software (6), which enabled determination of a relative deuterium level in a peptide at given H/D exchange time-point (Fig. S3B).

Collagenase activity assay. The wild-type MMP-1 and its mutants were used at a concentration of 10 nM to digest 4.5 µM collagen I in TNC buffer at 25 °C. Reactions were stopped at different time-points by the addition of SDS-PAGE loading buffer containing 20 mM EDTA. Products were analyzed by SDS-PAGE with 7.5 % total acrylamide under reducing conditions and the gels were stained with Coomassie Brilliant Blue R-250. The percentage cleavage was measured by densitometry using ImageScanner III (GE Healthcare) and Phoretics 1D (TotalLab) quantification software from which the initial rate of cleavage was calculated.

Complex formation and crystallization. The MMP-1(E200A)-collagen peptide complex for crystallization was formed by dissolving 2.2 mg of lyophilized peptide in 230 μ l of a concentrated MMP-1(E200A) solution (23.5 mg/ml protein in TNC buffer). After incubation for 30 minutes at room temperature, the mixture was subjected to size exclusion chromatography on a Superdex 75 HR10/30 column (GE Healthcare) at room temperature (Fig. S5). The MMP-1(E200A)-collagen peptide complex was concentrated to 8 mg/ml and screened for crystallization in vapor diffusion sitting drops using a Mosquito nanolitre robot (TTP LabTech). Clusters of thin needles grew after 2-3 days using 0.1 M Tris-HCl pH 8.5, 2% (v/v) Tacsimate pH 8.0, 16% (w/v) PEG 3350 as precipitant. These crystals were used to generate a seed stock using the Seed Bead kit (Hampton Research) according to the manufacturer's protocol. Single needle-shaped crystals of a few μ m thickness were obtained by microseeding crystallization drops pre-equilibrated in 0.1 M Tris-HCl pH 8.5, 8-11% (v/v) Tacsimate pH 8.0, 10-12.5% (w/v) PEG 3350. The crystals were flash-frozen in liquid nitrogen after a brief soak in mother liquor supplemented with 20% glycerol.

Crystal structure determination. Diffraction data were collected at 100 K on the microfocus beam line I24 at the Diamond Light Source (Oxfordshire, UK). Many crystals were screened to identify a single good crystal, from which all data were collected. To minimize radiation damage, a fresh crystal volume was exposed after each 20° of data collected, yielding a total of 140° of usable data. The data were processed with MOSFLM (www.mrc-lmb.cam.ac.uk/harry/mosflm) and programs of the CCP4 suite (7). The MMP-1-collagen structure was solved by molecular replacement with PHASER (8) using the human MMP-1 structure (PDB entry 2CLT) as a search model. After refinement with CNS (9), the electron density map calculated from the correctly positioned search model showed weak density for the collagen triple helix. A collagen peptide with poly-Gly-Ala-Ala sequence was constructed based on PDB entry 2WUH and positioned with PHASER. The model was completed using O (10) and refined with CNS (Table S2). Omit maps were used extensively to assign the correct register of the three collagen chains. The register of the leading chain passing through the active site cleft is defined unambiguously by the strong electron density of the Arg(P5'L) side chain. The two MMP-1(E200A)-collagen complexes in the asymmetric unit are very similar and tight non-crystallographic symmetry restraints were applied throughout the refinement. The only deviations from non-crystallographic symmetry are observed for the first three collagen triplets, which are not part of the collagen II sequence and do not interact with MMP-1(E200A).

1. Chung L, et al. (2000) Identification of the (183)RWTNNFREY(191) region as a critical segment of matrix metalloproteinase 1 for the expression of collagenolytic activity. *J Biol Chem* 275:29610-29617.
2. Seyer JM, Hutcheson ET, Kang AH (1976) Collagen polymorphism in idiopathic chronic pulmonary fibrosis. *J Clin Invest* 57:1498-1507.
3. Raynal N, et al. (2006) Use of synthetic peptides to locate novel integrin α 2 β 1-binding motifs in human collagen III. *J Biol Chem* 281:3821-3831.

4. Leo JC, et al. (2010) First analysis of a bacterial collagen-binding protein with collagen Toolkits: promiscuous binding of YadA to collagens may explain how YadA interferes with host processes. *Infect Immun* 78:3226-3236.
5. Chung L, et al. (2004) Collagenase unwinds triple-helical collagen prior to peptide bond hydrolysis. *EMBO J* 23:3020-3030.
6. Weis DD, Engen JR, Kass IJ (2006) Semi-automated data processing of hydrogen exchange mass spectra using HX-Express. *J Am Soc Mass Spectrom* 17:1700-1703.
7. The CCP4 suite: programs for protein crystallography (1994). *Acta Crystallogr D Biol Crystallogr* 50:760-763.
8. McCoy AJ, et al. (2007) Phaser crystallographic software. *J Appl Crystallogr* 40:658-674.
9. Brunger AT, et al. (1998) Crystallography & NMR system: A new software suite for macromolecular structure determination. *Acta Crystallogr D Biol Crystallogr* 54:905-921.
10. Jones TA, Zou JY, Cowan SW, Kjeldgaard M (1991) Improved methods for building protein models in electron density maps and the location of errors in these models. *Acta Crystallogr A* 47:110-119.
11. Iyer S, Visse R, Nagase H, Acharya KR (2006) Crystal structure of an active form of human MMP-1. *J Mol Biol* 362:78-88.

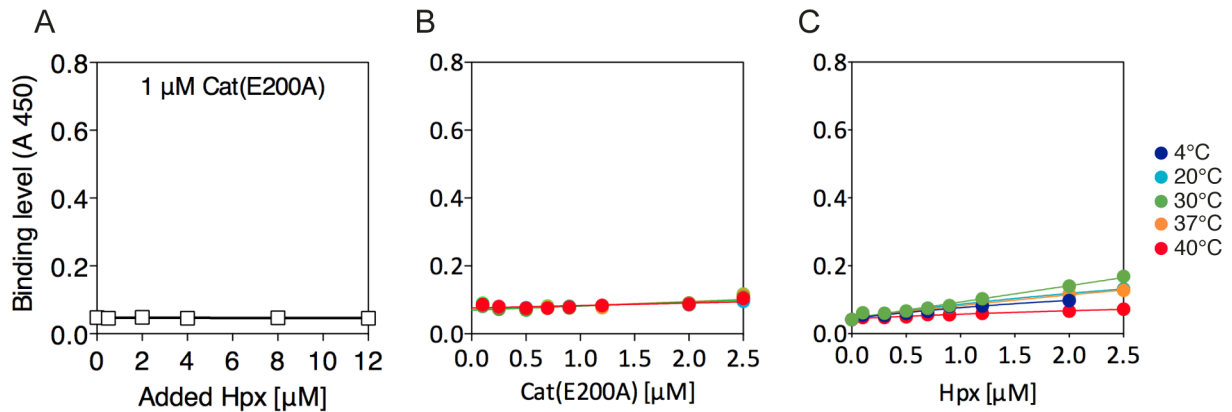


Fig. S1. Binding of the individual domains of MMP-1(E200A) to immobilized collagen I. (A) Cat(E200A) domain in the presence of increasing concentrations of the Hpx domain. (B) Cat(E200A) domain at increasing temperatures. (C) Hpx domain at increasing temperatures. All data points are triplicate average with SD smaller than a point size.

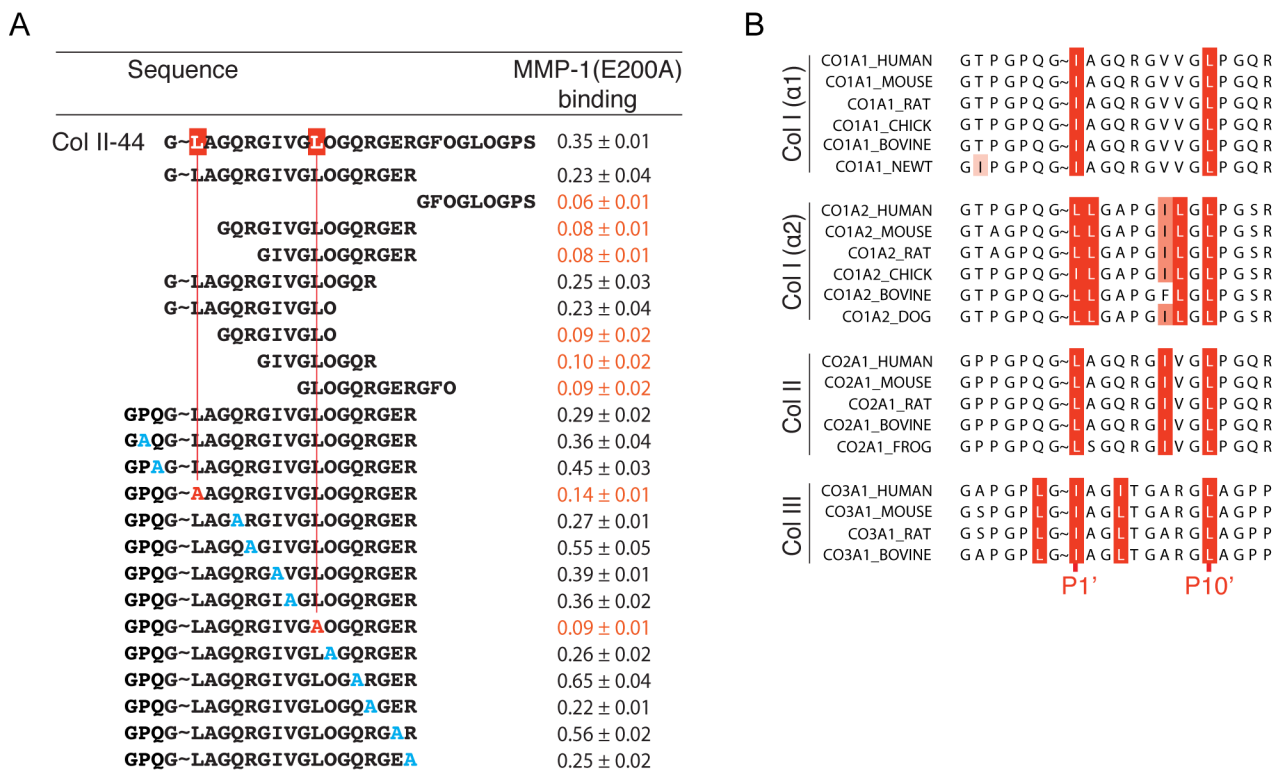


Fig. S2. Identification of the MMP-1(E200A) binding site in collagen II. (A) Binding of MMP-1(E200A) to truncated and alanine-substituted (shown in blue) derivatives of peptide Col II-44. Binding results are expressed as mean A_{450} values ± standard deviations from three independent experiments. Low binding data are shown in red text; O, hydroxyproline. (B) Sequence alignment of interstitial collagens I, II and III from different species in the proximity of the collagenase-cleavage site. Sequences are derived from cDNA. Leu and Ile residues are highlighted in red, and residues at P1' and P10' subsites are indicated. ~, Bond cleaved by collagenases.

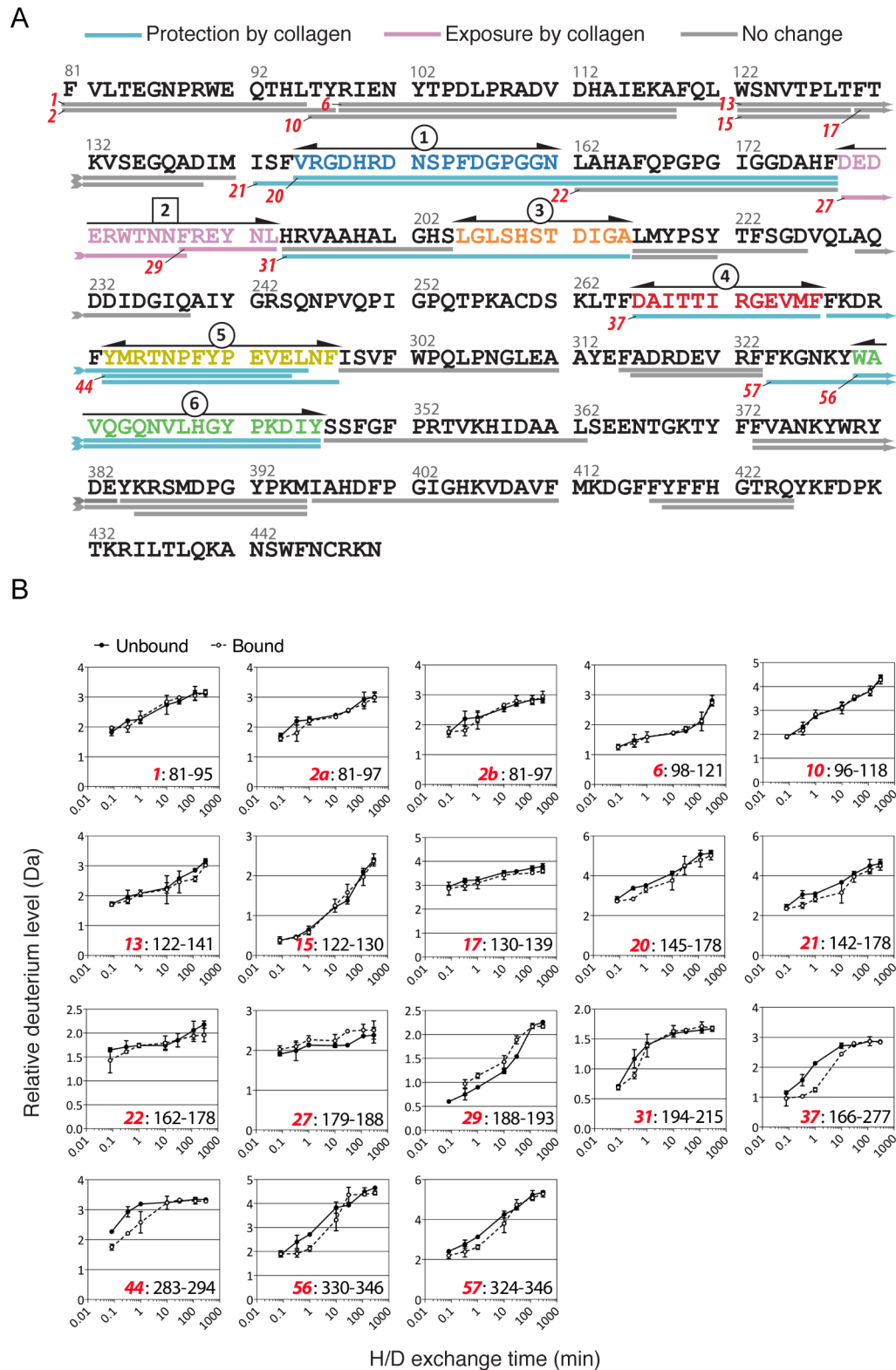


Fig. S3. Collagen I footprint on MMP-1(E200A) determined by H/DXMS. (A) Sites protected from deuterium incorporation (1 and 3-6, circled) or showing enhanced deuterium incorporation (site 2, square) upon collagen binding are indicated in the MMP-1(E200A) sequence. Site numbering and color coding corresponds with Fig. 2A, where the sites are mapped onto the crystal structure of MMP-1(E200A). All analyzed peptides are shown as bars below the sequence. Numbers in red refer to peptide numbers listed in

Table S1. (B) H/D exchange time-course analyses of selected MMP-1(E200A) peptic peptides; Unbound, free MMP-1(E200A); Bound, MMP-1(E200A) bound to collagen. Quantification of the exchange in MS spectra was performed using HX-Express software (6). Centroid (average) mass of each isotopic pattern was computed, which allowed determination of a relative deuterium level (*rdl*) in a peptide at given H/D exchange time-point by the following formula: $rdl = m - m_0$, where m is the average mass after H/D exchange and m_0 is the unexchanged average mass. Data are plotted by averaging results of two or three independent experiments. The numbers in red shown with sequence delimiters correspond to the peptide numbers in A; 2a and 2b denote different ions of the same peptide.

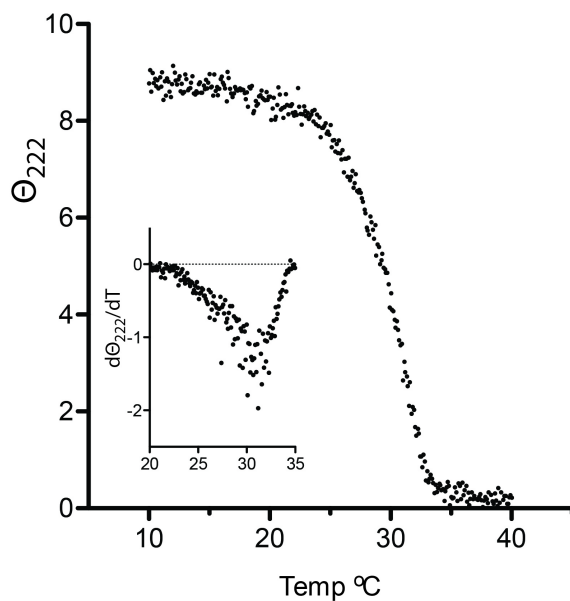


Fig. S4. Melting curve of collagen peptide used for co-crystallization with MMP-1(E200A) determined by circular dichroism (CD). The thermal transition of collagen peptide (10 μ M) in TNC buffer was determined in a Jasco 815 CD instrument at 222 nm with a 0.1 cm pathlength. Temperature was increased at 0.1 $^{\circ}$ C/min. The first derivative of the smoothed melting curve is shown in the inset. Θ , ellipticity.

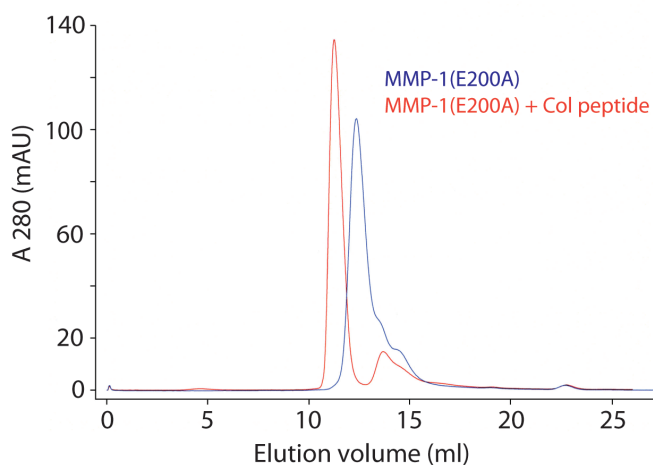


Fig. S5. Solution binding of MMP-1(E200A) to the collagen peptide. Analytical size exclusion (Superdex 75) chromatograms of the free MMP-1(E200A) and its complex with the collagen peptide.

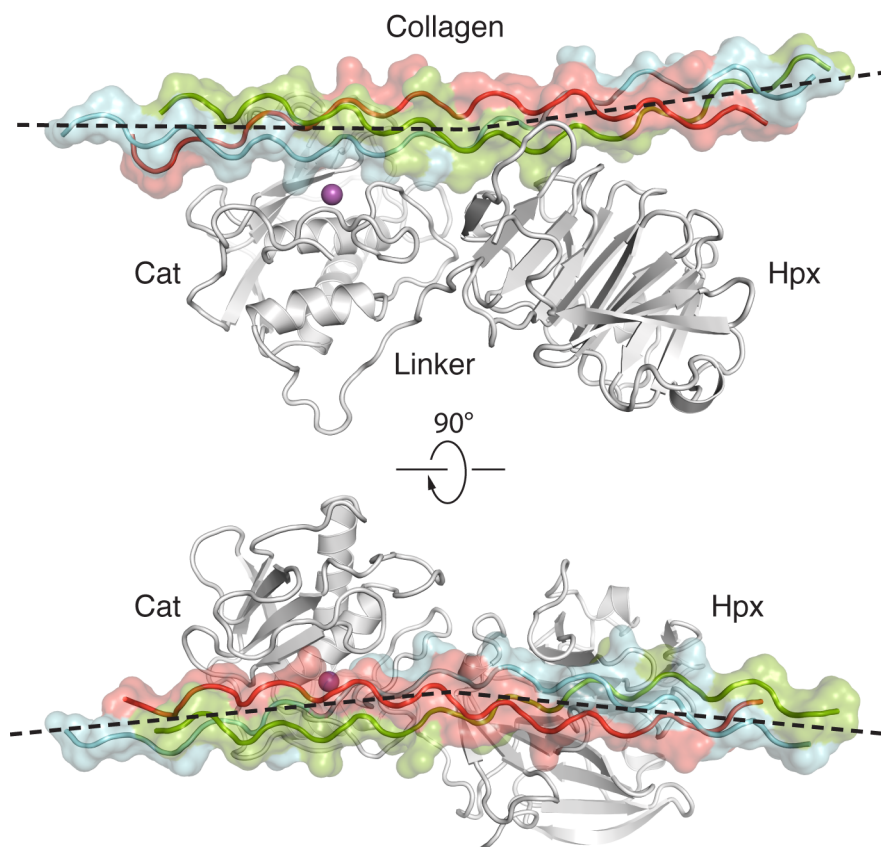


Fig. S6. Overall structure of the MMP-1(E200A)-collagen peptide complex and collagen bending. The collagen chains are colored cyan (L), green (M) and red (T). The dashed lines indicate the helix axes in the N- and C-terminal regions of the collagen peptide, which is bent by $\sim 10^\circ$ halfway between the Cat and Hpx domains. A magenta sphere represents the active-site zinc ion.

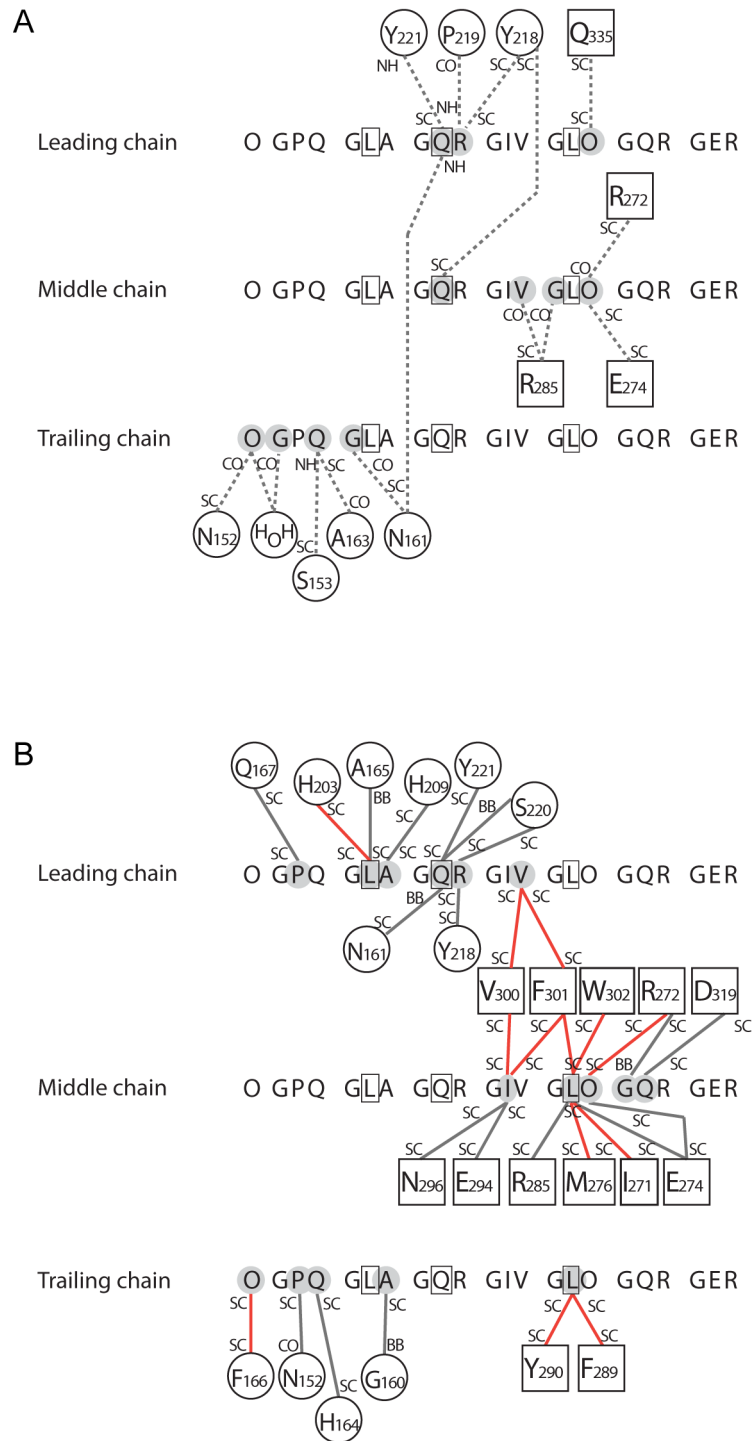


Fig. S7. Schematic representation of MMP-1-collagen interactions. MMP-1 residues are shown as circles (Cat domain) or squares (Hpx domain). Collagen subsites P1', P4' and P10' are boxed. (A) Hydrogen bonds (dashed lines) between MMP-1 and collagen. (B) Contacts of 4 Å distance or less (solid lines) between MMP-1 and collagen. Hydrophobic contacts are emphasized by red lines. BB, backbone; CO, main-chain carbonyl oxygen; NH, main-chain amide nitrogen; SC, side chain.

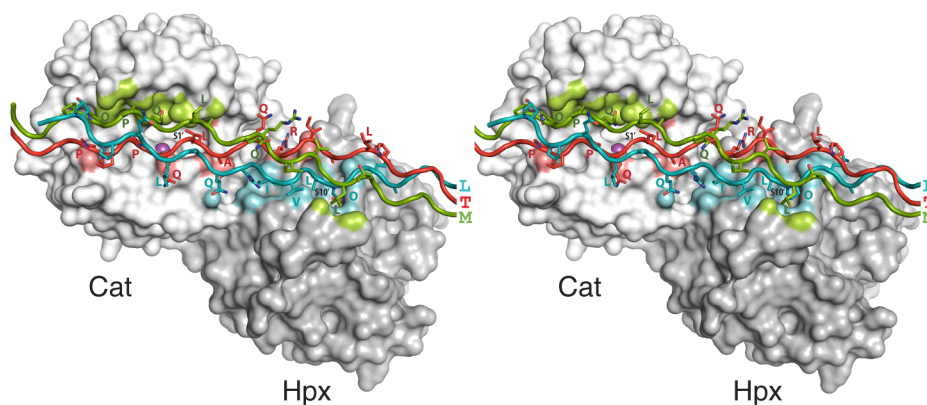


Fig. S8. Model of the putative productive complex. The collagen chains are in cyan (L), green (M) and red (T). The MMP-1(E200A) surface areas within 4 Å distance of the L, M and T chains are colored correspondingly. Collagen side chains are shown as sticks and are labeled.

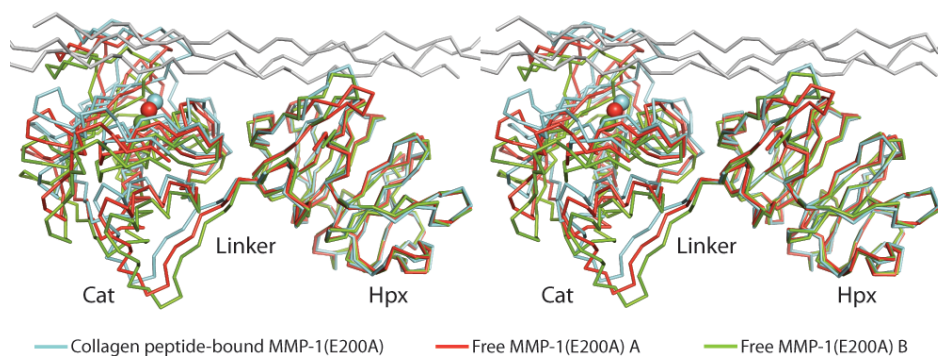


Fig. S9. Inter-domain flexibility in MMP-1. Shown is a stereoview of a superposition of the two crystallographically independent molecules of free MMP-1(E200A) (11) (molecule A, red; molecule B, green) and the MMP-1(E200A)-collagen peptide complex (MMP-1, cyan; collagen, gray). The structures were superimposed on the Hpx domains using Pymol.

Table S1. MMP-1(E200A) peptic peptides identified by nano-LC-Q-TOF and/or MALDI-Q-TOF MS/MS for H/D exchange analyses.

No.	Start-End	Sequence	Observed m/z = (M+z)/z	MALDI	M (experimental)	M (theor.)
1	81-95	FVLTEGNPRWEQTHL	609.75 - 609.79; 914.16	1826.93	1826.23 - 1826.34	1825.91
2	81-97	FVLTEGNPRWEQTHLTY	1046.25	2091.03	2090.49	2090.02
3	82-97	VLTEGNPRWEQTHLTY		1943.9	1942.89	1942.95
4	98-116	RIENYTPDLPRADVDAIE	742.19; 556.9 - 556.92		2223.54 - 2223.65	2223.09
5	98-118	RIENYTPDLPRADVDAIEKA	808.56 - 808.57	2423.24	2422.67 - 2422.69	2422.23
6	98-121	RIENYTPDLPRADVDAIEKAFQL	703.58-703.6; 703.75	2811.43	2810.38; 2810.98	2810.44
7	104-118	PDLPRADVDAIEKA	549.74		1646.2	1645.84
8	105-115	DLPRADVDAI	407.57		1219.69	1220.61
9	96-116	TYRIENYTPDLPRADVDAIE	-	2488	2487	2487.2
10	96-118	TYRIENYTPDLPRADVDAIEKA	672.75		2686.99	2686.34
11	131-141	TKVSEGGADIM	589.43 - 589.93		1176.84 - 1177.84	1177.56
12	127-141	PLTFTKVSSEGGADIM	-	1636.81	1635.8	1635.82
13	122-141	WSNVPLTFTKVSSEGGADIM	1112.77 - 1112.78	2224.06	2223.53	2223.09
14	122-129	WSNVPLT	917.62 - 917.7		916.61 - 916.7	916.47
15	122-130	WSNVPLTF	532.75 - 532.78		1063.49 - 1063.55	1063.53
16	130-138	FTKVSSEGQA	483.73 - 483.74		965.45 - 965.47	965.48
17	130-139	FTKVSSEGGAD	541.25 - 541.26; 541.39		1080.51; 1080.76	1080.51
18	130-141	FTKVSSEGGADIM	663.05 - 663.49	1325.62	1324.09 - 1324.96	1324.63
19	145-161	VRGDHRDNPFDGPGGN	599.59 - 599.60	1796.79	1795.78	1795.8
20	145-178	VRGDHRDNPFDGPGGNLAHAFQPGPGIGGDAHF	868.1 - 868.12	3469.67	3468.47 - 3468.66	3468.61
21	142-178	ISFVRGDHRDNPFDGPGGNLAHAFQPGPGIGGDAHF	-	3816.99; 3817.10	3815.98; 3816.09	3815.79
22	162-178	LAHAFQPGPGIGGDAHF	564.59 - 564.61	-	1690.75 - 1690.81	1690.82
23	179-187	DEDERWTNN	-	1178.47	1177.46	1177.46
24	179-190	DEDERWTNNFRE	-	1610.67	1609.66	1609.68
25	179-193	DEDERWTNNFREYNL	667.62	2000.85	1999.84	1999.87
26	188-198	FREYNLHRVAA	-	1375.71	1374.7	1374.72
27	179-188	DEDERWTNNF	663.25 - 663.27	-	1324.48 - 1324.52	1324.53
28	189-198	REYNLHRVAA	-	1228.64	1227.63	1227.65
29	188-193	FREYNL	421.20 - 421.22	-	840.38 - 840.42	840.41
30	194-214	HRVAAHELGHSLGSLHSTDIG	-	2136.09 Glu -> Ala (E) [-58.01]	2135.08	2135.1
31	194-215	HRVAAHELGHSLGSLHSTDIGA	736.53 Glu -> Ala (E) [-58.01]	2207.13 Glu -> Ala (E) [-58.01]	2206.58	2206.14
32	194-204	HRVAAHELGHSL	385.87 Glu -> Ala (E) [-58.01]	-	1154.59	1154.61
33	208-216	SHSTDIGAL	450.72	-	899.42	899.43
34	216-226	LMYPSYTFSGD	640.75 - 640.76	-	1279.49 - 1279.50	1279.54
35	230-238	AQDDIDIGIQ	487.71; 974.61 - 974.66	-	973.4; 973.6 - 973.65	973.47
36	266-276	DAITIRGEVM	603.29 - 603.31; 603.46	1205.59	1204.56 - 1204.61	1204.61
37	266-277	DAITIRGEVMF	676.81 - 677.0	1352.67; 1368 ox(M) [+16]	1351.6 - 1351.99	1351.68
38	266-273	DAITIRG	423.73 - 423.74	-	845.44 - 845.47	845.46
39	267-277	AITIRGEVMF	619.33 - 619.34	-	1236.65	1236.65
40	270-277	TIRGEVMF	476.73 - 476.75	-	951.44 - 951.48	951.48
41	277-282	FFKDRF	430.23	-	858.44	858.44
42	277-281	FFKDR	356.77 - 356.78	-	711.53 - 711.55	711.33
43	278-295	FKDRFYMRNPFYPEVEL	784.68	-	2351.03	2351.14
44	283-294	YMRTNPFYPEVE	773.30 - 773.35	1545.7; 1561 ox(M) [+16]	1544.69	1544.7
45	283-295	YMRTNPFYPEVEL	829.86 - 829.88	1658.79	1657.78	1657.78
46	283-297	YMRTNPFYPEVELNF	960.63 - 960.64	1919.88	1919.25 - 1919.27	1918.89
47	283-296	YMRTNPFYPEVELN	886.88 - 886.9	-	1771.74 - 1771.79	1771.82
48	298-311	ISVFWPQLPNGLA	-	1602.79 dox(W) [+31.99]	1601.78	1601.81
49	313-323	YEFADRDEVR	-	1446.66	1445.65	1445.66
50	315-323	FADRDEVR	358.52 - 358.53; 577.78 - 577.93	1154.52; 1154.55	1153.53 - 1153.84	1153.55
51	316-323	ADRDEVR	-	1007.48	1006.47	1006.48
52	316-329	ADRDEVRFFKGNKY	-	1744.86	1743.85	1743.87
53	315-329	FADRDEVRFFKGNKY	-	1891.84	1890.83	1890.94
54	315-322	FADRDEVR	336.5; 504.24	-	1006.47; 1006.48	1006.48
55	347-362	SSFQFPRTVKHIDAAL	582.77	-	1745.28	1744.93
56	330-346	WAVQGNVHLHGYPKDIY	-	1987.98	1986.97	1987
57	324-346	FKGNKYWAVQGNVHLHGYPKDIY	682.09	-	2724.33	2724.38
58	330-338	WAVQGNV	507.76	-	1013.5	1013.53
59	352-362	PRTVKHIDAAL	610.85	-	1219.68	1219.7
60	363-372	SEENTGKTYF	588.22 - 588.41	1175.52	1174.42 - 1174.8	1174.51
61	363-371	SEENTGKTY	514.71	-	1027.41	1027.45
62	373-383	FVANKYWRVDE	497.53 - 497.55; 745.81 - 745.83	1490.67; 1522.69 dox(W) [+31.99]	1489.58 - 1489.66	1489.7
63	373-384	FVANKYWRVDEY	551.91	1653.76	1652.69 - 1652.75	1652.76
64	373-395	FVANKYWRVDEYKRSMDPGYPKM	-	2944.37; 2944.42	2943.36; 2943.41	2943.38
65	373-385	FVANKYWRVDEYK	-	1653.76 Lys-loss (C-term) [-128.09]	1652.75	1652.76
66	382-395	DEYKRSMDPGYPKM	572.91	-	1715.71	1715.76
67	384-395	YKRSMDPGYPKM	491.54 - 491.57; 491.69	1488 ox(M) [+16]	1471.6 - 1471.68; 1472.04	1471.7
68	385-395	KRSMDPGYPKM	437.2 - 437.21	1309.63	1308.59 - 1308.62	1308.63
69	396-409	IAHDFPGIGHKVDVA	492.9 - 492.91	1476.76	1475.69 - 1475.75	1475.75
70	396-411	IAHDFPGIGHKVDVAF	431.46; 574.93 - 575.09; 861.92	1722.89	1721.78 - 1722.28	1721.89
71	417-425	YFFHGTTRQ	-	1202.57	1201.56	1201.57
72	418-425	YFFHGTTRQ	528.25 - 528.26	1055.5	1054.48 - 1054.5	1054.5
73	419-423	FFHGT	608.43	-	607.43	607.28

Numbers in red refer to the peptides for which H/D exchange kinetics is shown in Figure S2. Many peptides were identified in differently charged forms, especially with the electrospray ionization (ESI) method. Several ions were detected multiple times, and the ranges of their observed mass-over-charge (m/z) values are shown. M, peptide mass; M(experimental) was calculated as follows: $M = ((m/z) z) - z$.

Table S2. Crystallographic statistics of the MMP-1(E200A)-collagen peptide structure

Data collection	
Space group	P2
Unit cell dimensions	
a, b, c (Å)	76.67, 102.24, 80.73
α , β , γ (°)	90, 103.76, 90
Asymmetric unit content	2 MMP-1(E200A)-collagen complexes
Solvent content (%)	57
Resolution (Å)	20-3.0 (3.16-3.00) ^a
R _{merge}	0.128 (0.400)
<I/ σ (I)>	5.0 (2.2)
Completeness (%)	86.8 (77.9)
Multiplicity	1.7 (1.6)
Refinement	
Resolution (Å)	20-3.0
Reflections	20982
Protein atoms	7368
Solvent atoms	8 Ca ²⁺ + 4 Zn ²⁺ + 7 H ₂ O
R _{work} /R _{free}	0.211/0.273
R.m.s. deviation bonds (Å)	0.008
R.m.s. deviation angles (°)	1.4
Ramachandran plot (%) ^b	79.2, 18.5, 2.2, 0.1

^aValues in parentheses are for the highest resolution shell.

^bPercentage of residues in core, allowed, generously allowed and disallowed regions (program PROCHECK).